AD-A093 286 IBM THOMAS J WATSON RESEARCH CENTER YORKTOWN HEIGHTS NY F/G 7/4
HIGH RESOLUTION ELECTRON ENERGY LOSS AND SURFACE ENHANCED RAMAN--ETC(U)
OCT 80 J E DEMUTH, P N SANDA, J M WARLAUMONT N00014-77-C-0366
UNCLASSIFIED TR-12 NL

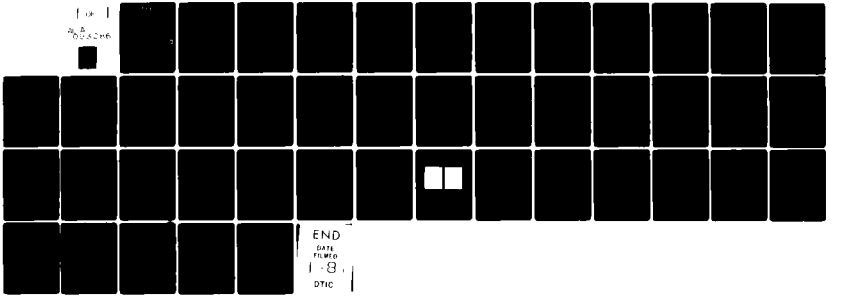

END
DATE FILMED
1-81
DTIC

AD A093286

LEVEL II

12

OFFICE OF NAVAL RESEARCH

Contract N00014-77-C-0366

Task No. NR 056-123

TECHNICAL REPORT NO.12

High Resolution Electron Energy Loss and Surface Enhanced Raman Studies of Pyridine and Benzene on Ag(111)

by

J.E. Demuth, P.N. Sanda, J.M. Warlaumont, J.C. Tsang

and K. Christmann

to appear in the

"Proceedings of the Surface Vibrations Conference"

Namur, Belgium

September 1980

IBM T.J. Watson Research Center

Yorktown Heights, New York 10598

DTIC ELECTE DEC 23 1980 D C

October 27, 1980

Reproduction in whole or in part is permitted for any purpose of the United States Government

This document has been approved for public release and sale; its distribution is unlimited

DDC FILE COPY

80 12 22 099

UNCLASSIFIED

SECURITY CLASSIFICATION OF THIS PAGE (When Data Entered)

REPORT DOCUMENTATION PAGE		READ INSTRUCTIONS BEFORE COMPLETING FORM
1. REPORT NUMBER: Technical Report No. 12	2. GOVT ACCESSION NO.: AD-A093 286	3. RECIPIENT'S CATALOG NUMBER
4. TITLE (and Subtitle): High Resolution Electron Energy Loss and Surface Enhanced Raman Studies of Pyridine and Benzene on Ag(111),		5. TYPE OF REPORT & PERIOD COVERED
		6. PERFORMING ORG. REPORT NUMBER
7. AUTHOR(s): J.E. Demuth, P.N. Sanda, J.M. Warlaumont, J.C. Tsang and K. Christmann		8. CONTRACT OR GRANT NUMBER(s): N00014-77-C-0366
9. PERFORMING ORGANIZATION NAME AND ADDRESS: IBM T.J. Watson Research Center, P.O. Box 218, Yorktown Heights, New York 10598		10. PROGRAM ELEMENT, PROJECT, TASK AREA & WORK UNIT NUMBERS
11. CONTROLLING OFFICE NAME AND ADDRESS: Office of Naval Research, Chemistry Program Office, Arlington, VA 22217		12. REPORT DATE: October 27, 1980
		13. NUMBER OF PAGES
14. MONITORING AGENCY NAME & ADDRESS (if different from Controlling Office): TR-12		15. SECURITY CLASS. (of this report): Unclassified
		15a. DECLASSIFICATION/DOWNGRADING SCHEDULE

16. DISTRIBUTION STATEMENT (of this Report)

Approved for Public Release; Distribution Unlimited.

17. DISTRIBUTION STATEMENT (of the abstract entered in Block 20, if different from Report)

18. SUPPLEMENTARY NOTES

Preprint; to appear in the "Proceedings of the Surface Vibrations Conference," Namur, Belgium, September 1980.

19. KEY WORDS (Continue on reverse side if necessary and identify by block number)

Raman, Surfaces, Chemisorption, Pyridine, Benzene, Silver, Structure, Bonding, Plasmons

20. ABSTRACT (Continue on reverse side if necessary and identify by block number)

High resolution electron energy loss (EELS), UV photoemission, (UPS), low energy electron diffraction (LEED), Auger electron, and thermal desorption spectroscopic techniques have been applied to characterize the bonding, molecular orientation and vibrations of pyridine and benzene on clean Ag(111). These results are used to interpret the surface enhanced Raman spectra of these molecules adsorbed on a clean, well-defined single crystal Ag(111) surface containing a smooth periodic modulation (1 micron wavelength, ~500 Å amplitude)

DD FORM 1 JAN 73 1473

UNCLASSIFIED

SECURITY CLASSIFICATION OF THIS PAGE (When Data Entered)

which permits optical coupling to surface plasmons-polaritons. We observe enhanced Raman scattering (RS) for chemisorbed species only when we are at appropriate incidence angles so as to excite surface plasmons. Coverage-dependent RS studies indicate a long-range field enhancement of $\sim 10^2$ for physisorbed layers and a mode-selective, short-range enhancement of $\sim 10^4$ for the symmetric ring breathing mode of pyridine. This short-range enhancement only occurs for pyridine coverages slightly above $\sim 3 \times 10^{14}$ molecules/cm^2 where changes in the UPS spectra and our UPS derived uptake-rates are also observed. Similar coverage-dependent effects are also observed in UPS and EELS for chemisorbed pyridine on the ideal Ag(111) surface. These as well as LEED results showing the modulated surface to be predominately (~90%) single crystal Ag(111), encourage us to directly compare the results obtained for the two surfaces.

From EELS we determine that chemisorbed pyridine π-bonds and lies flat on the surface of Ag(111) to within $\sim 5^\circ$ but at higher chemisorption coverages ($> 3 \times 10^{14}$ molecules/cm^2) becomes nitrogen-lone-pair-bonded, inclined $\sim 55^\circ$ to the surface and rotated $\sim 30^\circ$ about the $C_{2v}(\sigma d)$ point group symmetry. We thereby relate the strong short-range enhancement observed in RS to the occurrence of nitrogen lone-pair-bonding and the inclination of chemisorbed pyridine to Ag(111). Both the mode selectivity and structure sensitivity for chemisorbed pyridine are shown to be consistent with the recent surface plasmon-polariton model of enhanced Raman scattering by Kirtley, Jha, and Tsang. Also observed in RS are additional vibrations which we associate with pyridine bound to step sites and at or near graphitic carbon impurities.

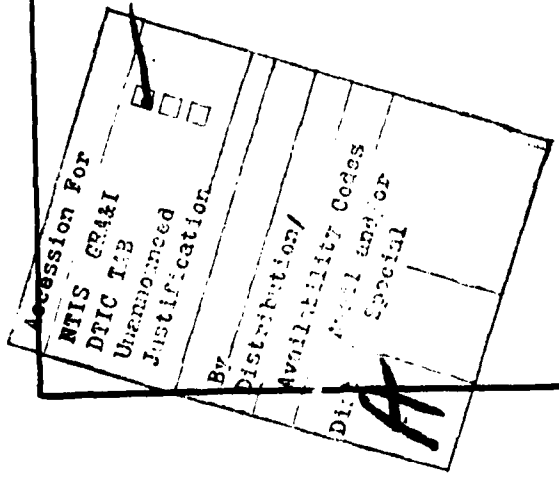

HIGH RESOLUTION ELECTRON ENERGY LOSS AND SURFACE ENHANCED RAMAN STUDIES OF PYRIDINE AND BENZENE ON Ag(111).

J. E. Demuth, P. N. Sanda,* J. M. Warlaumont,

J. C. Tsang and K. Christmann**

IBM Thomas J. Watson Research Center
P. O. Box 218, Yorktown Heights, NY 10598

Abstract: High resolution electron energy loss (EELS), UV photoemission, (UPS), low energy electron diffraction (LEED), Auger electron, and thermal desorption spectroscopic techniques have been applied to characterize the bonding, molecular orientation and vibrations of pyridine and benzene on clean Ag(111). These results are used to interpret the surface enhanced Raman spectra of these molecules adsorbed on a clean, well-defined single crystal Ag(111) surface containing a smooth periodic modulation (1 micron wavelength, ~ 500 Å amplitude) which permits optical coupling to surface plasmons-polaritons. We observe enhanced Raman scattering (RS) for chemisorbed species only when we are at appropriate incidence angles so as to excite surface plasmons. Coverage-dependent RS studies indicate a long-range field enhancement of $\sim 10^2$ for physisorbed layers and a mode-selective, short-range enhancement of $\sim 10^4$ for the symmetric ring breathing mode of pyridine. This short-range enhancement only occurs for pyridine coverages slightly above $\sim 3 \times 10^{14}$ molecules/cm^2 where changes in the UPS spectra and our UPS derived uptake-rates are also observed. Similar coverage-dependent

effects are also observed in UPS and EELS for chemisorbed pyridine on the ideal Ag(111) surface. These as well as LEED results showing the modulated surface to be predominately (~90%) single crystal Ag(111), encourage us to directly compare the results obtained for the two surfaces.

From EELS we determine that chemisorbed pyridine π-bonds and lies flat on the surface of Ag(111) to within ~5° but at higher chemisorption coverages ($> 3\times10^{14}$ molecules/cm^2) becomes nitrogen-lone-pair-bonded, inclined ~55° to the surface and rotated ~30° about the C_{2V} symmetry axis. Benzene is found to π-bond and has vibrations characteristic of a $C_{3V}(\sigma d)$ point group symmetry. We thereby relate the strong short-range enhancement observed in RS to the occurrence of nitrogen lone-pair-bonding and the inclination of chemisorbed pyridine to Ag(111). Both the mode selectivity and structure sensitivity for *chemisorbed* pyridine are shown to be consistent with the recent surface plasmon-polariton model of enhanced Raman scattering by Kirtley, Jha, and Tsang. Also observed in RS are additional vibrations which we associate with pyridine bound to step sites and at or near graphitic carbon impurities.

---

† Work supported in part by the office of Naval Research.

* Affiliated with Cornell University, Ithaca, NY.

** Present address: Institut für Physikalische Chemie der Universität München

München, West Germany

I. Introduction

The occurrence of large enhancements in Raman cross sections for molecules adsorbed at metal surfaces in electrochemical cells [1], discontinuous films [2], colloidal suspensions [3], tunnel junctions [4], and in ultra high vacuum [5-10] is well-documented. The nature and origin of this enhancement mechanism is unclear and currently in dispute. Two predominating viewpoints exist: (a) that surface roughness and the creation of collective surface excitations are important [3,4,5,8,11]; (b) that specific ad-atom sites or arrangements of coadsorbed atoms form a type of "surface-complex" which is a strong or resonant Raman scatterer [9,12,13]. Such differing viewpoints may both be correct and could arise from the diversities of the systems under investigation. This possibility highlights a major problem of most all current surface enhanced Raman studies: *there is a lack of detailed information about the structure of the surface, its cleanliness, or the nature of bonding or orientation of the adsorbed species on the surface.*

The purpose of our study is twofold: (1) to characterize the nature of bonding, the molecular geometry and the vibrations of a variety of chemisorbed molecules on a clean Ag(111) single crystal surface using several surface science techniques; and (2) to perform Raman measurements on these same systems under as identical conditions as possible. From the correlation of these two results we hope to understand more concerning the nature of surface enhanced Raman. In particular, we perform our Raman measurements on a clean single crystal Ag(111) surface which has a weak periodic profile

(10,000 Å periodicity, ~500 Å amplitude) built into the crystal surface. We find as observed previously for tunnel junction structures [4] that enhanced Raman scattering also occurs from this type of controlled roughness surface. Thus our Raman studies are intended to address questions relating to the mechanism of enhanced Raman scattering on roughened surfaces [4,11] specifically where surface plasmon-polaritons occur.

Here we choose to present our results for two adsorbates, pyridine and benzene, the former being fairly extensively studied in other enhanced Raman studies [1,5,7,9]. Benzene is chosen for comparison to pyridine as it has a similar size, shape and vibrations as pyridine but lacks the nitrogen-lone-pair orbital. From previous studies [14,16] different adsorption geometries are expected for these two molecules. Indeed, we determine that while both benzene and pyridine can π-bond and lie flat on Ag(111), pyridine can nitrogen-lone-pair bond at higher chemisorption coverages. We observe a direct correspondence between these structural effects and our observed Raman signals. Evidence for similar structural effects has been presented for the cyanopyridines in previous electrochemical studies [17]. We also observe coverage dependent and mode selective enhancements which are consistent with a recent surface plasmon polariton theory by Kirtley, Jha and Tsang [18].

II. Experimental Procedures

The experimental measurements were performed in three separate ultra-high vacuum (UHV) systems (base pressure $< 1 \times 10^{-10}$ Torr). The first

(turbomolecular pumped) system described elsewhere [19] allows UPS, low-energy electron diffraction (LEED), Auger (AES) and TDS to be performed. The second (ion and titanium sublimation - pumped) system is mobile and permits *in situ* LEED, AES and Raman scattering measurements to be performed. The third (ion- and titanium-sublimator-pumped) system permits EELS and work function change measurements.

The electron optics for EELS consists of two sets of 2.5 cm hemispherical deflection analyzers with associated focusing optical elements [20] so as to allow the monochromatization, reflection from a sample (total scattering angle of 90°) and energy analysis of a well-defined (< 0.2 mm dia.), collimated (< 1°), low-energy 2-100 eV electron beam. For the specular reflection of a 3 eV beam off of Ag(111), we have routinely obtained a total system resolution of 65-75 cm^{-1} (8-9 mV) with peak counting rates of 10^6 cps. Although both the monochromator and analyzer are in a fixed position, the sample rotation is arranged so as to enable the observation of specular ($\theta_{in} = \theta_{out}$) as well as off-specular ($\theta_{in} \neq \theta_{out}$) scattering events in the plane of incidence. Such off-specular angle dependent measurements are needed to assess the magnitude of resonant electron scattering and other non-dipole scattering processes in the specular scattering direction. Although such measurements have been performed and *must be* considered in the analysis of our specular scattering results, we do not present them here.

For the EELS experiments we use an ideal flat Ag(111) crystal. The Ag(111) surface was prepared by standard mechanical [19] and chemical

polishing [21], then annealed and sputter cleaned as determined by AES. This clean, well-ordered Ag(111) sample was then inserted into the EELS system where further sputter cleaning and annealing was performed. Work-function change measurements performed in both UHV systems as well as EELS spectra served to verify surface cleanliness in the HREEL system. The final clean samples were mirror smooth and showed minimal optical defects or irregularities. All chemisorption experiments in the EELS system were done at temperatures of ~140K as monitored by a chromel alumel thermocouple.

In order to observe Raman signals from adsorbed species, we have intentionally modified the topography of a Ag(111) crystal. This surface contains a small amplitude, approximately sinusoidal modulation (amplitude ~500 Å), which provides a well-defined surface periodicity (wavelength = 10,000 Å) to allow optical coupling to surface plasmon-polaritons, while maintaining minimal deviation from a flat Ag(111) surface. The Ag(111) sample was cut from the same boule as the aforementioned crystal, mechanically and chemically polished, then annealed and sputter-cleaned in UHV. A final chemical polish left the surface with a mirror-like finish, free of etch pits. The 10,000 Å periodic surface modulation was then fabricated into a 4×4 mm area of the 8×6 mm face of the crystal, with the modulation wave vector $\vec{K}_s$ oriented along to the (110) direction. This structure was fabricated by first creating a photoresist pattern on the sample using X-ray lithography techniques followed by chemical polishing to remove about 3000 Å of material in the unmasked regions (50%). The photoresist was then dissolved and the

sample repetitively Argon ion sputter-etched and annealed to ~500K in UHV for cleaning. This processing also reduces the higher order fourier components [22] of the profile and results in a sinusoidal-like surface (valleys slightly wider than the peaks) with a 10,000 Å wavelength and ~500 Å amplitude as estimated by the LEED beam profiles. Photographs of the LEED pattern from the flat and "modulated" region of this sample are shown in Fig. 1. The modulated region of the sample shows a well-defined, low background LEED pattern, comparable to the flat portion of the sample. Satellite lobes are observed in the beam profiles, which indicated a distribution of steps and terraces parallel to $\vec{K}_s$. The peak in this distribution corresponds to a terrace width to step height ratio of about 10 to 1. The intensity of the main peak relative to the side lobes indicates that roughly 90% of the surface is of (111) orientation. Although such LEED features serve as a guide to the general nature and condition of the surface, they do not provide specific information on all types of defects and their distributions.

UPS measurements were performed on both samples. As determined from these measurements, we observe negligible differences in the UPS ionization levels of adsorbates between the flat and topologically modified surfaces. We also find no change in the chemisorption properties for pyridine or benzene when the sample is between 80 and 140K - the limiting values of sample temperatures in the Raman and EELS systems, respectively.

Reagent grade pyridine and benzene (99.9%) and their deuterated counterparts (99 atom % D) were used in these experiments. Sample dosing

was done via the chamber ambient and directly monitored with an ion gauge. All exposures cited here are in units of Langmuirs, L (1L = 10^6 Torr – sec) and have been corrected by a gauge factor of 5.8 [23]. The dosages required to produce both the compressional phase of pyridine and first physisorbed layers were the same in all three UHV systems.

III. EELS Results

Our EELS results indicate that a structural phase transformation occurs for chemisorbed pyridine on Ag(111) at an exposure of ~0.5L. In Fig. 2 we show the EELS vibrational loss spectra for chemisorbed pyridine before (solid line) and after (dotted line) this transition. Here, the relative intensities of the CH deformation modes between 400-850 cm^{-1} strongly change, especially when compared to the relative IR-adsorbances [24,25] also shown in Fig. 2. Such IR absorbances directly reflect the dipole scattering intensities of a randomly oriented pyridine molecule and can be compared to EELS results for specular scattering ($\theta_i = \theta_0$). The transition is more striking in the coverage dependent spectra shown in Fig. 3. We note that the strong decrease in intensity of the ~700 cm^{-1} feature above 0.5L exposure indicates that at least 93% of the lower coverage phase converts to a new structure. This 700 cm^{-1} feature becomes strong again above 1L exposures when pyridine starts to physisorb as determined from our UPS results [8,26].

In Fig. 4 we show the spectra of deuterated pyridine below and above this phase change, as well as a schematic drawing of the molecular orienta-

tions which we attribute to each phase. Note in Fig. 4 that the symmetric ring breathing mode at 965 cm^{-1} is clearly resolved and nearly identical to the liquid phase value of 962 cm^{-1}. From our angle-dependent studies, we also observe strong non-dipole scattering from the losses at 2260(3040) cm^{-1}, 1540(1570) cm^{-1} and ~820(~1000) cm^{-1} for deuterated (normal) pyridine. Finally, we find that the vibrational frequencies for both phases of normal or deuterated pyridine are identical within our experimental uncertainties of ± 5 cm^{-1}.

In order to obtain structural information, the vibrational losses must be assigned to the vibrational modes of the molecule. Such an assignment would seem formidable based upon the relatively poor resolution of EELS and the fact that pyridine is of low symmetry and has 27 IR-active modes [27]. Fortunately, we find that we can straightforwardly assign most all the observed vibrational losses since (a) only a fraction of the 27 free-molecule modes have significant dipole scattering cross sections (i.e., IR absorbances, see Figs 2 and 4); and (b) pyridine is weakly chemisorbed and leads to weakly perturbed vibrations ($\Delta\nu_{avg} = \pm 6$ cm^{-1}) relative to liquid pyridine. These assignments are tabulated and described elsewhere [26].

Based upon the mode assignments we consider the (dipole-derived) scattering intensities of in-plane and out-of-plane vibrations relative to the IR-absorbances to obtain structural information. Although our analysis is described elsewhere [26], we briefly comment on the essential points here. The low coverage phase shows intense, out-of-plane, CH deformation vibra-

tions at 700 cm^{-1} (525 cm^{-1}) and 400 cm^{-1} (360 cm^{-1}) for normal (deuterated) pyridine which becomes suppressed after the phase change. With this phase change the in-plane, CH-deformation vibration at 610 cm^{-1} (560 cm^{-1}) become more intense. From our angle-dependent measurements we find that these forementioned in-plane and out-of-plane modes are dominated by dipole scattering in the specular direction which thereby permits their use in a structural analysis. As a result of the "surface selective rule" [28], the relative intensities of these in-plane and out-of-phase vibrations indicate that the molecule becomes more inclined to the surface above 0.5L exposure. Based upon our UPS results [8,26] as well as other chemical arguments and results [15,16], the inclined phase of pyridine has the nitrogen end of the molecule directed into the surface. Further the in-plane, CH-deformation vibration at 1440 cm^{-1} (1305 cm^{-1}) which is polarized largely perpendicular to the C_{2V} symmetry plane of the molecule [27] increases intensity relative to the in-plane deformation mode at 610 cm^{-1} which are symmetric about the C_{2V} symmetry plane. This implies that a rotation also occurs about the inclined C_{2V} symmetry axis of the molecule after this phase transformation occurs.

From a quantitative analysis of the such dipole scattering intensities relative to the IR intensities of liquid pyridine [25], we have determined that the low coverage phase (< 0.4L) lies flat on Ag(111) to within 5° and the high coverage chemisorbed phase (> 0.6L but < 1.0L) lies inclined ~55° to

the surface and rotated ~30° about the molecular C_{2V} symmetry axis. Unlike a previous analysis of EELS data to obtain quantitative geometric information [29], our analysis does not depend on evaluating dynamic charges for which the detailed transmission function of the analyzers must be evaluated. Instead our analysis relies on analyzing *relative* intensities of close-lying vibrational losses where we can reasonably assume that our analyzer transmission function is constant. Thus, our EELS results provide evidence that *chemisorbed* pyridine initially π-bonds to Ag(111) for exposures < 0.5L and at higher coverages forms a compressed structure which is nitrogen-lone-pair bonded and inclined to the surface.

Our photoemission results are also consistent with these conclusions for chemisorbed pyridine as we observe the π_1 -orbital derived ionization feature and lose the ionization feature having nitrogen-lone-pair character when the molecules becomes inclined [26]. Our TDS results show that this inclined phase is less strongly bound to the surface than the π-bonded phase by ~2Kcal/mole and that even the more strongly bonded phase desorbs below ~210K. Interestingly, we also find evidence that the first layers of condensed pyridine lie "flat" on top of the compressed high coverage phase of chemisorbed pyridine (see Fig. 3).

Our EELS results for benzene adsorption on Ag(111) indicate only one chemisorbed phase. The EELS spectra of chemisorbed benzene is shown in Fig. 5 where we also show the IR absorbances for liquid benzene [25]. EELS results have previously been presented for benzene on Ni(111) and Pt(111)

[11] and also have been discussed from a point-group-symmetry theoretic viewpoint [30]. Unlike these previous results on transition metals the vibrations of chemisorbed benzene on Ag(111) are remarkably similar to liquid benzene and allow a unique opportunity to directly relate group theoretic-concepts to EELS results.

From the relative intensities of the 1480 cm^{-1} or 3030 cm^{-1} in plane CH deformation or stretching vibration, and the out-of-plane CH-deformation vibration at 675 cm^{-1} we conclude that benzene lies π-bonded, flat on the surface. The losses observed at 675, 1000, 1155 and 3030 cm^{-1} can become (dipole) excited if the molecular symmetry is lowered to the $C_{3V}(\sigma d)$ point group from the D_{6h} point group of the free molecule (see ref. 30). These vibrations correspond to the a_1 modes which should be the *only* modes (dipole) excited under the surface selection rule [28]. The two weak modes at 1360 cm^{-1} and 1480 cm^{-1} must also be explained. The 1360 cm^{-1} loss may arise from an "impurity" (?) in our benzene as it is commonly observed in the IR spectrum [25], or *more likely* to the second harmonic of the intense 675 cm^{-1}, loss feature. The very intense 1480 cm^{-1}, peak in liquid benzene corresponds to an in-plane vibrations and may arise for chemisorbed benzene from "incomplete" surface screening of the image charge by the substrate (i.e., a weakening of the surface selection rule) or the occurrence of quadruple excitations. Fortunately, the 1155 cm^{-1} loss is unique to the $C_{3V}(\sigma d)$ point group, cannot be resonantly excited in the free molecule [31] and from our angle-dependent studies appears to arise from dipole scattering. This mode is

also extremely weak in liquid benzene [25] and would account for its weak intensity here. Thus, although many of the loss features which delineate the point group symmetry of adsorbed benzene are weak and of comparable intensity to resonance scattering features and incompletely screened parallel modes, we find the observed vibrations to be consistent with a $C_{3V}(\sigma d)$ point group symmetry. Such questions regarding the excitation mechanism or the totality of the surface selection rule underlay applying group theoretic concepts to determining adsorption site symmetry particularly if the new vibration associated with the reduced symmetry are weak. Unfortunately, one does not know *a priori* what the intensities of such features will be.

IV. Raman Scattering Results

Enhanced Raman scattering signals were observed at surface plasmon-polariton resonance [4,31], which was obtained by varying the orientation of the incident radiation with respect to $\vec{K}_s$. For the data presented here, we have used p-polarized incident radiation and oriented the sample so that $\vec{K}_s$ is in the plane of incidence. The angle of incidence was set to the minimum in intensity of the direct reflected beam, which corresponds to maximal surface plasmon-polariton excitation. As expected, there was no Raman scattered signal observed from the flat (control) portion of the sample or when plasmon resonance conditions were not achieved. With present signal to noise ratios and sampling times we would need an enhancement factor for chemisorbed pyridine of $\sim 5 \times 10^2$ to observe any Raman signals above our noise levels.

The features found to be observable in the Raman spectrum for chemisorbed pyridine on our "clean" modulated Ag(111) surface occur between 850 and 1050 cm^{-1} as shown as a function of exposure in Fig. 6a. Compared to the liquid phase spectra, for which the symmetric (991 cm^{-1}) and the asymmetric (1030 cm^{-1}) ring breathing modes are of about equal intensity, these spectra show selective enhancement of the symmetric breathing mode for chemisorbed pyridine. At higher exposures (~20L) the asymmetric ring-breathing mode becomes observable, and at yet higher exposures (>44 L), characteristic of very thick layers of pyridine, we start to observe additional Raman scattering with similar relative intensities as liquid pyridine.

For chemisorbed pyridine on "clean" Ag(111), the carbon ring deformation modes in the 1300 to 1600 cm^{-1} range could not be detected. Such features may be masked by the broad peaks at 1350 and 1500 cm^{-1} due to trace amounts of graphitic carbon [33,34]. Such trace amounts of graphitic carbon always occurred in RS but were undetectable by AES. Also, prior to complete annealing, we observed an additional peak at 986 cm^{-1} which we associate with pyridine bound to step sites. Thus, we attribute the 990 cm^{-1} peak to chemisorbed pyridine on Ag(111) which is consistent with our EELS results. We have been unable to observe the CH stretching modes (near 3040 cm^{-1}) for chemisorbed pyridine.

In Fig. 6b we show Raman spectra obtained when greater amounts of graphitic carbon were observed in Raman but were still undetectable by AES. (As described elsewhere graphitic carbon has a very large Raman cross section

and can be readily detected in small quantities (~.01 monolayers) at plasmon-polariton resonance conditions [34]). For the 0.8L and first 2.6L spectra the graphitic carbon Raman signal is ~4× larger than our nominally clean Ag(111) surface (spectra shown in (a)) while in the second 2.6L exposure they are 10× more intense. As shown in Fig. 6b, the presence of graphitic carbon leads to additional Raman peaks at 1005 cm^{-1} in the chemisorption regime and at 1040 cm^{-1} for thicker condensed layers. These extra peaks are likely associated with pyridine interacting with the graphitic carbon but we cannot completely exclude the possibility of an overall degradation of the grating surface topography associated with long sputtering which was attempted (unsuccessfully) to reduce the of graphitic carbon. If the former is correct, then the Raman enhancement for pyridine-graphite/Ag is at least an order of magnitude higher than for pyridine on Ag. Although the occurrence of such impurities and their effect on RS are clearly important, we restrict further discussion to our RS studies on the "clean" Ag(111) surface.

Using our UPS results we have calibrated the relative coverages of pyridine on clean Ag(111) from the intensity of the adsorbate-derived ionization features and determine the coverage at which chemisorption stops and adsorption on top of this chemisorbed layer begins. This delineation between chemisorbed and physisorbed species is important, and is based upon the occurrence of different relaxation effects in UPS for the chemisorbed versus physisorbed molecule as described elsewhere [8,35]. Using coverage dependent Raman spectra as in Fig. 6a we determine the coverage dependence of the

990 cm^{-1} peak which is shown in Fig. 7. Here, we have calibrated our relative coverages in terms of monolayer equivalents - the coverage at which chemisorption is complete and condensation begins. We observe a strong signal starting about ~0.6 monolayers which increases less strongly above ~1 monolayer. Estimating the saturation coverage of pyridine to be $\sim 5 \times 10^{14}$ molecules/cm^2, as based on EELS results [26], and from comparisons to our Raman measurements on a known volume of liquid pyridine, we determine an enhancement for the first monolayer of $\sim 10^4$. At coverages above ~4 monolayers the enhancement per each additional monolayer remains at $\sim 10^2$.

These coverage dependent results are in agreement with a theoretical model by Kirtley, Jha and Tsang [18] which predicts two mechanisms contributing to the surface enhanced Raman scattering process for a molecule adsorbed on a sinusoidal grating. First, there is a long-range contribution, which extends several thousand Angstroms away from the surface, and is due to enhancement of the direct scattering intensity caused by the large electric field at surface plasmon-polariton resonance. This field enhancement is predicted by the theory to provide an increase in the Raman signal by a factor of 10^2 to 10^4. The second contribution is associated with a short-range mechanism, which is very localized to the surface. This enhancement arises from a modulation of the large oscillating charge density in the molecular layer at surface plasmon-polariton resonance, by the molecular vibrations, so

as to produce stokes shifted light at this modulation frequency. Here the surface plasmon-polariton is the intermediate state of a resonance Raman process. At atomic distances, this theory predicts a total combined Raman enhancement factor of between 10^4 and 10^6.

Our Raman scattering results for benzene show a different behavior than observed for pyridine. Namely, we do not observe any detectable signal until we have ~8 monolayer equivalents of benzene on the surface. At higher coverages we then start to observe a Raman spectra with similar relative intensities as in liquid benzene. The multilayer Raman signal is enhanced by a factor of $\sim 10^2$ as found for condensed pyridine. We again associated this with a field enhancement. We do not observe any enhancements $>10^2$ for chemisorbed benzene, a point we discuss later.

V. Discussion

Our Raman results show a strong ($\sim 10^4$) short-range enhancement for certain modes of chemisorbed pyridine which is ~ 50 times stronger than the expected long-range field enhancement. Our discussion here focuses on the factors which we can relate to this strong, short-range phenomena. In particular the similarities in chemisorption behavior of pyridine on Ag(111) and on our topologically modified Ag(111) surface encourages us to consider a direct comparison of the chemisorption results on these two surfaces. Namely, each adsorbate shows ionization levels and coverage dependent features in UPS which are similar on both surfaces, while pyridine additionally shows the onset

of the Raman signal where the structural phase transformation of pyridine occurs on the ideal Ag(111) surface. Such common features in the behavior of these adsorbates on the two surfaces imply that (a) large regions of Ag(111) surface occur on the "modulated" surface and (b) that defects do not totally disrupt the nature of adsorption on these "modulated" surfaces.

We find no evidence to conclude that defect sites on our modulated surface or the terrace edge atoms are themselves dominating the strong short-range enhancement. In fact, the lack of this enhancement off of surface plasmon-polariton resonance or on similar step density but nonmodulated Ag surfaces [5] strongly argues against these as the sole source of the enhancement. Further, Ag ad-atom sites which have been proposed as enhancement sites in other studies disappear above room temperature [6,7,10]. Our annealing of the sample well above room temperature would likely preclude such ad-atom sites on our surface. Indeed our observation of a sudden "turn" on of the Raman signal at higher chemisorption converges is contrary to the initially large signal observed on surfaces where ad-atoms are thought to play a role [9]. We thereby believe that the short range enhancement we observe (above our limits of sensitivity) is associated with the more general nature of our modulated surface.

We can consider a correlation of the adsorption properties of pyridine on the flat and modulated surface based on the "average" microscopic structure of each. Namely from our LEED results on the topologically modulated surface we expect a distribution of Ag(111) with an average terrace width of

~20 Å. In Fig. 8 we illustrate the atomic size of such a terrace and show how pyridine may π-bond to such a surface. Even considering the possibility that the pyridine molecules may bond differently at the step or kink sites of the terrace (i.e., the left side of Fig. 8) additional space remains on the terrace for adsorbed pyridine molecules to interact with a (111) surface and their neighboring molecules. We expect to observe largely the same coverage-dependent interactions on these (111)-terraces as found on Ag(111). We thereby associate the onset of the Raman signal in Fig. 7 with the inclination of chemisorbed pyridine and the occurrence of nitrogen lone-pair-bonding. The molecules located at the step or kink sites of the surface may also be effected during this transition as we observe the 986 cm^{-1} peak (see Fig. 6a). We also find that adsorption on these stepped Ag surfaces is reversible - unlike what is observed on the more reactive stepped transition metal surfaces [36].

Another important feature of our enhanced Raman scattering for chemisorbed pyridine is the mode selectivity. Namely, the symmetric ring breathing mode is selectively enhanced while for liquid or thick condensed layers of pyridine the symmetric and asymmetric modes are of comparable intensities. Any model of the enhancement mechanism must account for such mode selectivity.

For chemisorbed benzene, the lack of a detectable signal can be attributed to a lower enhancement factor which, by virtue of comparison to pyridine, we associate with the flat lying, π-bonded molecule. Namely, we might expect to see chemisorbed benzene since the Raman intensities of the ~990

cm^{-1} modes of liquid benzene and pyridine are comparable. However, as found for pyridine, the enhancement becomes large only when the molecule becomes inclined to the surface.

Several origins of the enhancement mechanism have been proposed [37] and we briefly comment on their consistency with our results. One can generally consider two related sources for the short-range enhancement: an electronic effect (e.g., a localized electronic excitation associated with chemisorption) and a physical effect (e.g., the orientation of the electric fields and the molecules on the surface). In relation to the former process we note that the symmetric-ring breathing mode is precisely the mode excited in resonant low energy electron scattering from gaseous pyridine and benzene [31,38]. Such a resonant state may couple to surface plasmon-polaritons and directly or indirectly provide the enhancement. However, this type of resonant state does not appear to be a *sufficient condition* for the enhancement since we do not observe a strong, short-range enhancement for chemisorbed benzene *even though we do observe the gas phase resonances for chemisorbed benzene* in EELS [39]. Further frequency dependent studies may help resolve the likelihood of this process.

The physical orientation of the molecule in the surface plasmon-polariton induced fields, with or without an image charge component [39], also fails to account for our results. Namely, a field enhancement only accounts for at most 3% of the observed signal while an image field enhance-

ment mechanism would predict comparable Raman intensities for both symmetric and asymmetric ring breathing modes. As previously mentioned a localized enhancement associated with bonding to ad-atoms on our silver surface would seem unlikely in view of our relatively severe annealing conditions. However, recent studies of pyridine on continuous and island Ag films evaporated at low temperature [9,10] also show preferential enhancement of the symmetric ring breathing mode.

Our experimental results appear to be consistent with the short-range surface plasmon-polariton enhancement mechanism proposed by Kirtley, Jha and Tsang [18]. Their enhancement contains both electronic and structural features. Namely, (a) certain molecular vibrations couple to the surface charge according to the nature of the bonding and (b) the final surface charge modulation can only occur *normal to the surface* and is thereby dependent on the orientation of the molecule on the surface. Thus, for pyridine we can relate the mode selectivity to the fact that the asymmetric ring breathing mode does not strongly modulate the surface charge density whereas the symmetric mode does. Such adsorbate-induced surface charge modulation at the surface likely occurs for π-bonded species as well but may be weaker or negated by the binding geometry or site symmetry. The details of such selection rules for surface plasmon-polariton enhanced Raman scattering are discussed in more detail elsewhere [41].

VI. Summary and Conclusions

We have used high resolution electron energy loss spectroscopy to determine the vibrations and molecular orientation of chemisorbed pyridine and benzene on Ag(111). Chemisorbed benzene is π-bonded having a point group symmetry of $C_{3V}(\sigma d)$. Pyridine also π bonds but undergoes a compressional phase transformation to form a more weakly bound, inclined, nitrogen-long-pair bonded phase of chemisorbed pyridine. We can relate these findings to Raman scattering results on a clean Ag(111)-oriented surface. We observe that the vibrations observed in *both* experiments on clean Ag(111) are very weakly perturbed from those of the free molecule. The symmetric ring breathing mode is within 3 cm^{-1} of its liquid phase value (RS for pyridine and EELS for d_5-pyridine). We also observe other frequencies for this mode in Raman which can be attributed to bonding at step sites (lower frequency) or to the presence of surface impurities (higher frequencies).

We find a strong structure dependence of our enhanced surface Raman signal for chemisorbed pyridine on clean Ag(111). Namely, we observe a $\sim 10^4$ enhancement of the 990 cm^{-1} mode when chemisorbed pyridine becomes inclined to the surface. For thicker layers of benzene or pyridine we observe little structural dependence and a factor of 10^2 weaker, longer-range field enhancement characteristic of randomized molecular orientations within this layer. We also observe a strong mode selective enhancement for chemisorbed pyridine. The observed enhancement occurs only at surface plasmon-polariton resonance conditions and appears to be well described within a

surface plasmon-polariton model [16]. Namely, both the mode selectivity and distance dependence of the enhancement we observe are consistent with the modulated surface dipole model of surface enhanced Raman scattering. Our results imply that only certain molecular vibrations and molecular orientations of a chemisorbed species on the surface will provide a large surface plasmon-polariton derived enhancement.

Acknowledgement: The authors wish to acknowledge useful discussions with J. R. Kirtley and S. S. Jha. We also thank J. A. Bradley for his technical assistance.

References

1. M. Fleishman, P. J. Hendra, and A. J. McQuillan, Chem. Phys. Lett. **26**, 163 (1974), D. L. Jeanmarie and R. P. Van Duyne, J. Electroanal. Chem. **84**, 1 (1977); B. Pettinger and U. Wenning, Chem. Phys. Lett. **56**, 253 (1978).

2. C. Y. Chen, E. Burstein and S. Lundquist, Solid State Commun. **32**, 63 (1979).

3. J. A. Creighton, C. G. Blatchford, and M. G. Albrecht, J. Chem. Soc., Faraday Transactions II **75**, 790 (1979); M. Kerker, O. Siiman, L. A. Blum and D. W. Wang, Applied Optics xx, xxx(1980).

4. J. C. Tsang, J. R. Kirtley, and J. A. Bradley, Phys. Rev. Lett. **43**, 772 (1979).

5. J. E. Rowe, C. V. Shank, D. A. Zwemer, C. A. Murray, Phys. Rev. Lett. **4**, 1770 (1980); D. A. Zwemer, C.V. Shank and J. E. Rowe, Chem. Phys. Lett. **73**, 201 (1980).

6. T. A. Wood and M. V. Klein, J. Vac. Sci. Technol. **16**, 459 (1979).

7. R. R. Smardzewski, R. J. Colton, J. S. Murday, Chem. Phys. Lett. **68**, 53 (1979).

8. P. N. Sanda, J. M. Warlaumont, J. E. Demuth, J. C. Tsang, K. Christmann and J. A. Bradley, to be published.

9. I. Pockerand and A. Otto, to be published.

10. H. Seki and M. Philpot, J. Chem. Phys., to be published.

11. M. Moskovits, J. Chem. Phys. **69**, 4159 (1978).

12. B. Pettinger, M. R. Philpolt, J. G. Gordon, III, J. Chem. Phys. xx, xxx (1980).

13. M. Fleishman, private communication.

14. S. Lehwald, H. Ibach and J. E. Demuth, Surface Sci. **78**, 577 (1978).

15. B. J. Bandy, D. R. Lloyd and N. V. Richardson, Surface Sci. **89**, 344 (1979).

16. F. P. Netzer, E. Bertel and J. A. D. Matthew, Surface Sci. **92**, 43 (1980).

17. C. S. Allen and R. P. Van Duyne, Chem. Phys. Lett. **63**, 455 (1979).

18. J. R. Kirtley, S. S. Jha and J. C. Tsang, Solid State Comm. **35**, n 7 (1980); S. S. Jha, J. R. Kirtley and J. C. Tsang, Phys. Rev. B., Oct. 15 (1980).

19. J. E. Demuth, Surf. Sci. **69**, 365 (1977).

20. J. A. Simpson and C. E. Kuyatt, Rev. Sci. Inst. **38**, 103 (1967).

21. H. J. Levinstein and W. H. Robinson, J. Appl. Phys. **33**, 3149 (1962).

22. P. S. Maiya and J. M. Blakely, Appl. Phys. Lett.**7**, 60 (1965).

23. This corresponds to the gauge-correction factor for benzene as supplied with our Varian ion gauge.

24. L. Corrsin, B. Fox and R. C. Lord, J. Chem. Phys. **21**, 1170 (1953).

25. D. J. Pouchart, *Aldrich Library of Infrared Spectra* (Aldrich Chem. Co., Wisconsin, 1975).

26. J. E. Demuth, K. Christmann and P. N. Sanda, Chem. Phys. Lett., to appear.

27. D. A. Long and E. L. Thomas, Trans. Far. Soc. **59**, 783 (1963).

28. D. Sokcevic, Z. Lenac, R. Brado and M. Sujic, Z. Phys. B **28**, 273 (1977).

29. H. Ibach, H. Hopster and B. Sexton, Appl. Surface Sci. **1**, 1 (1977).

30. N. V. Richardson, Surface Sci. **87**, 622 (1979).

31. S. F. Wong and G. J. Schulz, Phys. Rev. Lett. **35**, 1429 (1975).

32. A. Girlando, M. R. Philpolt, D. Heitmann, J. D. Swalen and R. Santo, J. Chem. Phys. **72**, 5187 (1980).

33. M. R. Mahoney, M. W. Howard and R. P. Cooney, Chem. Phys. Lett. **71**, 59 (1980).

34. J. C. Tsang, J. E. Demuth, P. N. Sanda and J. R. Kirtley, Chem. Phys. Lett., to appear.

35. J. E. Demuth and D. E. Eastman, Phys. Rev. Lett. **32**, 1123 (1974); J. Vac. Sci. and Technol. **13**, 283 (1976).

36. G. A. Somorjai, J. Vac. Sci. and Technol. **1**, 250 (1974).

37. See for example, E. Burstein, C. Y. Chen and S. Lundquist, in *Proceedings of Joint US-USSR Symposium on the Theory of Light Scattering in Condensed Matter*, eds. J. L. Birman, H. Z. Cummings and H. K. Reband (Plenum Press, NY, 1980) p. 479.

38. I. Nenner and G. J. Schulz, J. Chem. Phys. **62**, 1747 (1975).

39. J. E. Demuth, to be published.

40. F. King, R. P. Van Duyne and G. C. Schulz, J. Chem. Phys. **69**, 4472 (1978).

41. J. E. Demuth, P. N. Sanda, J. R. Kirtley, J. C. Tsang and S. S. Jha, to be published.

FIGURE CAPTIONS

1. LEED photograph of the Ag(111) surface (T = 80K) at 146 eV on the grating (right) and off the grating (left) The photo on the right of the modulated surface has been overexposed to more clearly show the weaker satellite spots.

2. Vibrational loss spectra of pyridine on Ag(111) at two coverages above and below the compressional phase transition. The IR absorbances [24,25] are shown below for comparison where the * levels are reduced by 1/3.

3. Coverage dependence of the vibrational spectra of chemisorbed pyridine (< 1.0L exposure). The spectra taken at a 2×10^{-7} Torr ambient pressure corresponds to the onset of condensation and the formation of the first physisorbed layers.

4. Vibrational loss spectra of deuterated pyridine on Ag(111) at coverages above and below the compressional phase transformation. The IR absorbances [24, 25] are shown below for comparison where the * levels are reduced by 1/3. The insert besides each spectra schematically represents the geometry characteristic of each phase (see text).

5. Vibrational loss spectra for benzene on Ag(111) and the corresponding IR absorbances [24]. Note that the peak at 1038 cm^{-1} is the ν_{14}, e_{iu} mode which *does not* correspond to the 1000 cm^{-1} loss feature. The

1000 cm^{-1} IR peak is very weak and is *not* observable on this scale.

6. Raman scattering signal as a function of increasing coverage for two conditions: (a) the nominally clean topologically modulated Ag(111) surface, and (b) with increased carbon contamination (see text).

7. Raman scattering intensity for the 990 cm^{-1} peak as a function of coverage (in monolayer equivalents - see text). The insert shows the detailed low coverage behavior. (λ = 5145Å)

8. Schematic model of the topologically modulated, stepped Ag(111) surface used in the Raman experiments. An average terrace width of 20 Å is determined from the LEED results (Fig. 1). The adsorbed pyridine molecules are shown to scale, bound to some arbitrary but largely constant local bonding sites.

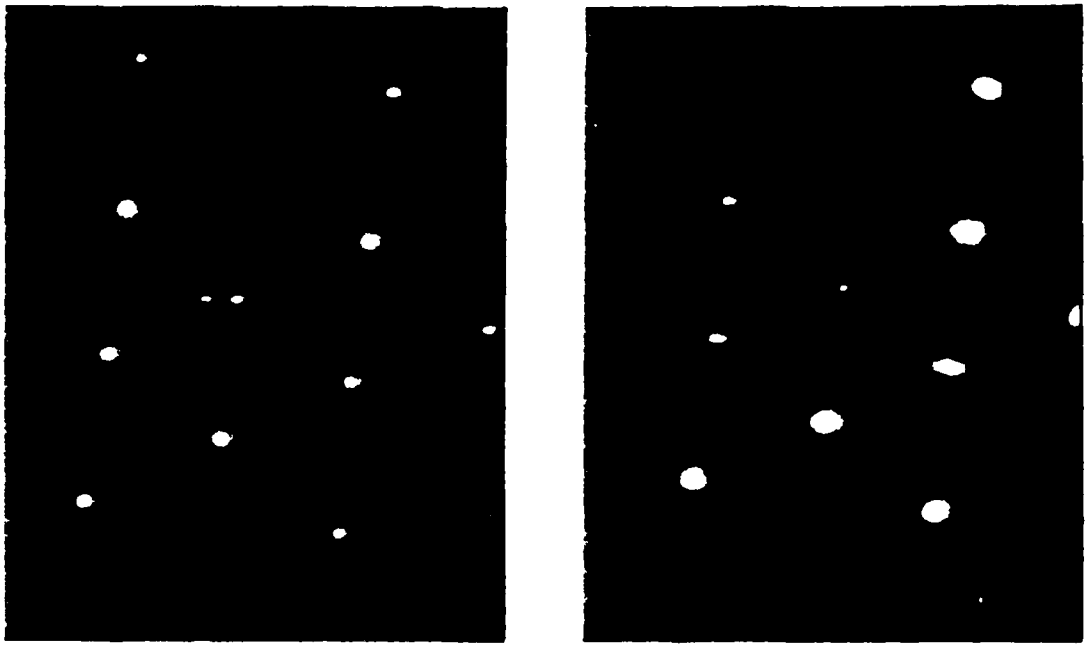

Fig 1
Dainouth et al.

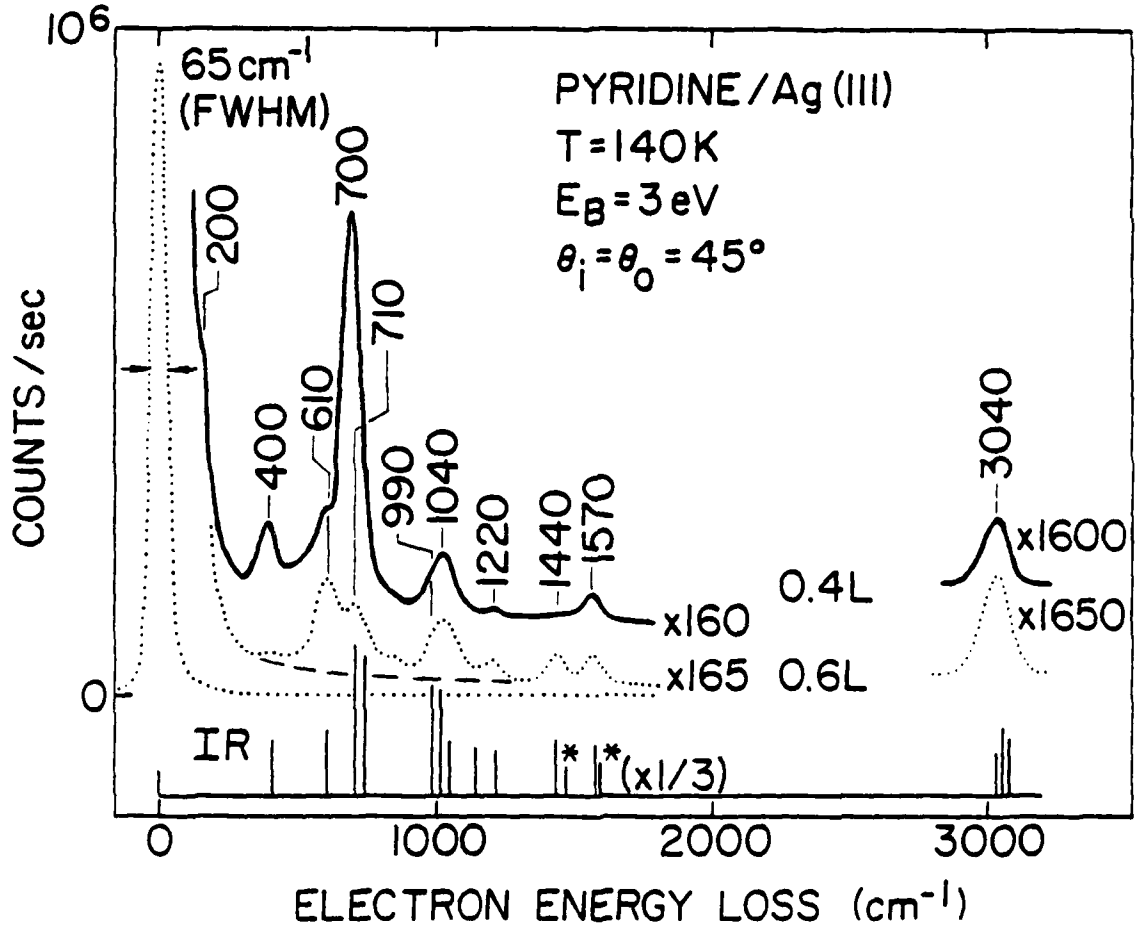

FIG 2
Demuth et al.

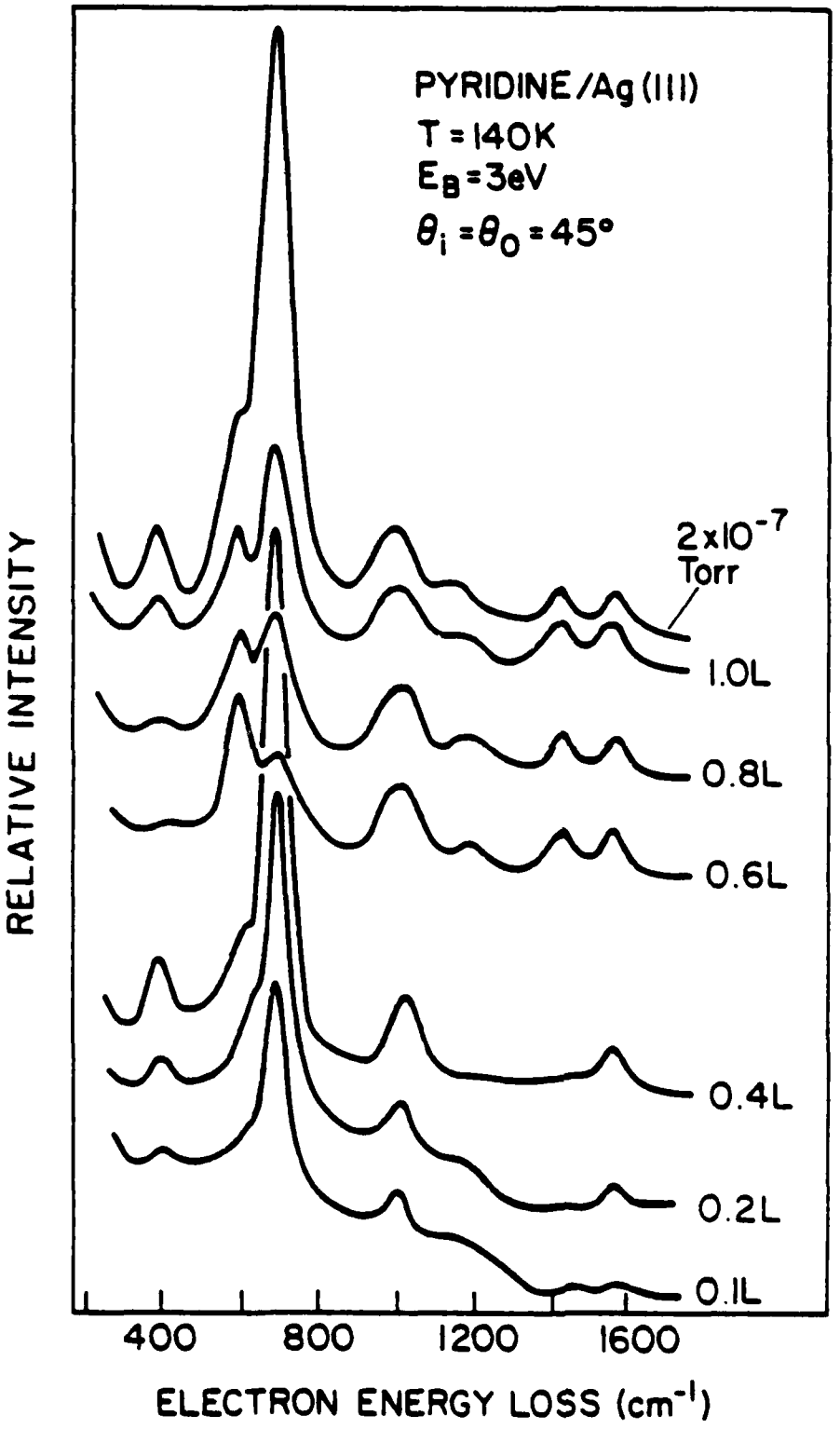

FIG 3
DEMUTH, ET. AL

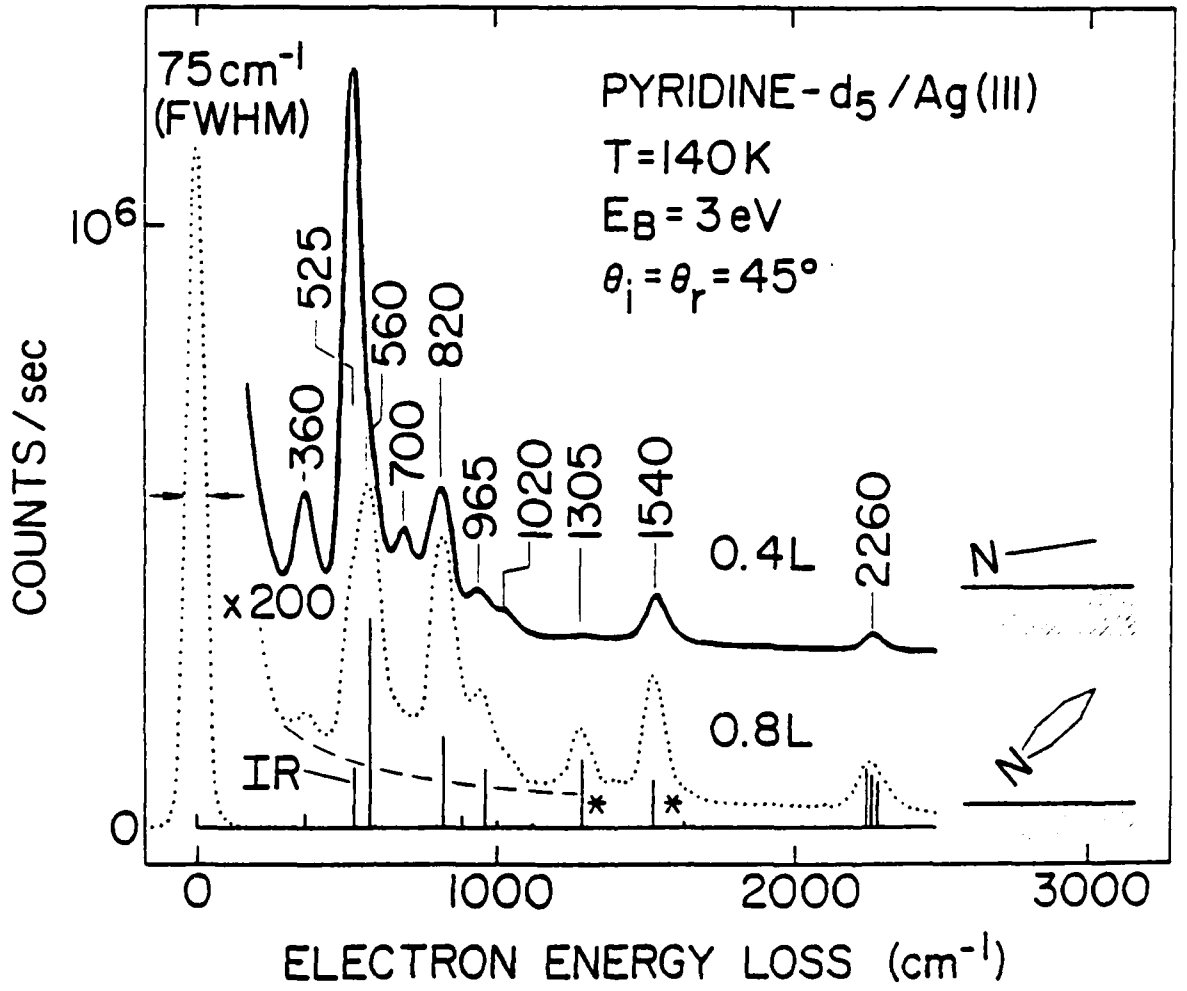

FIG 4
Demuth et al

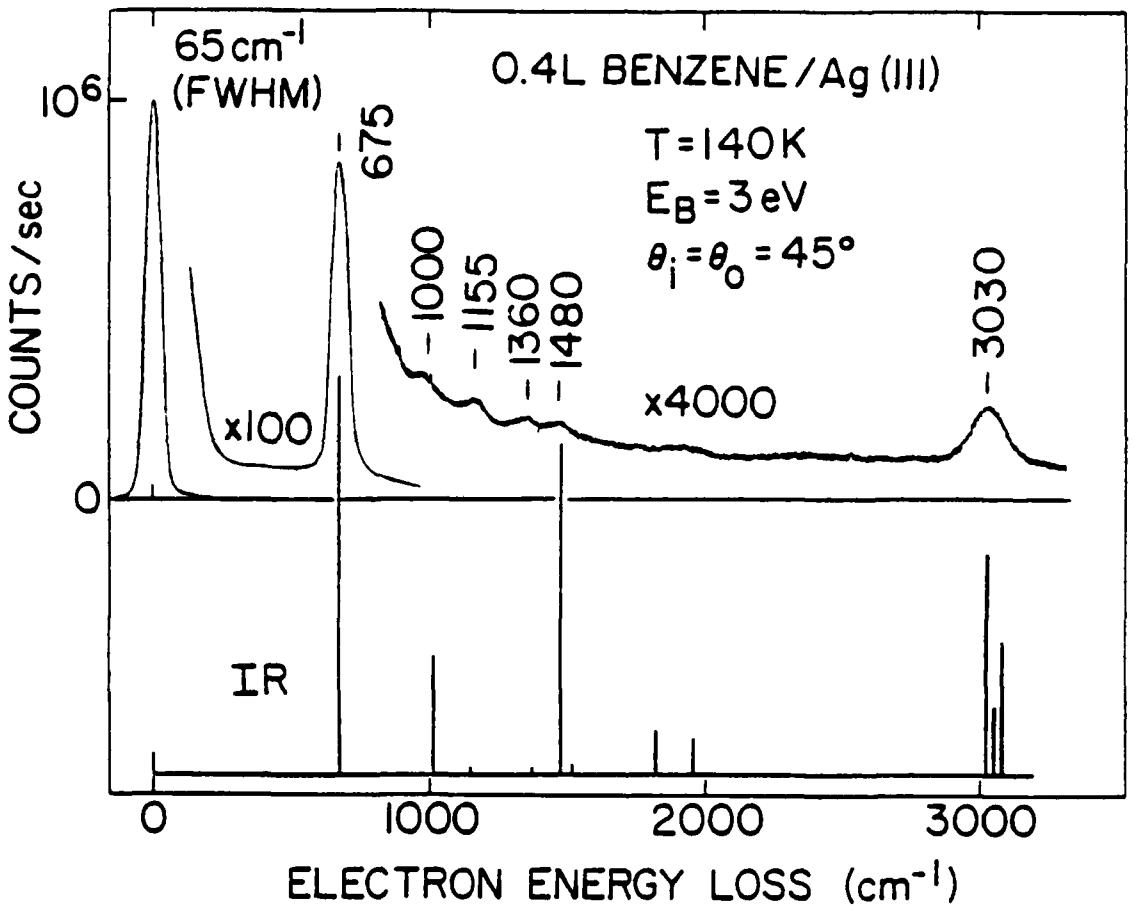

FIG 5
Demuth et al

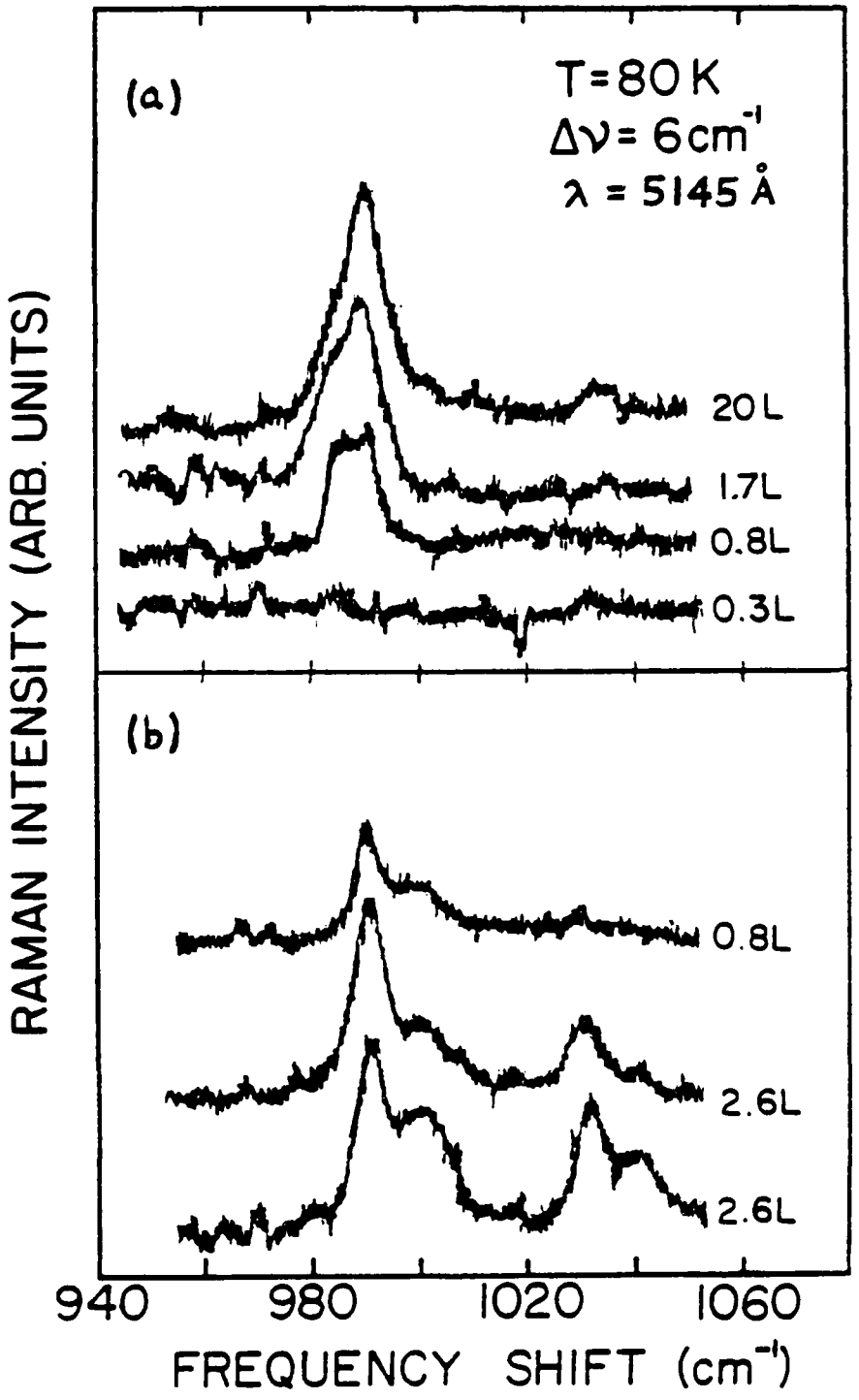

FIG 6
Demuth, et al

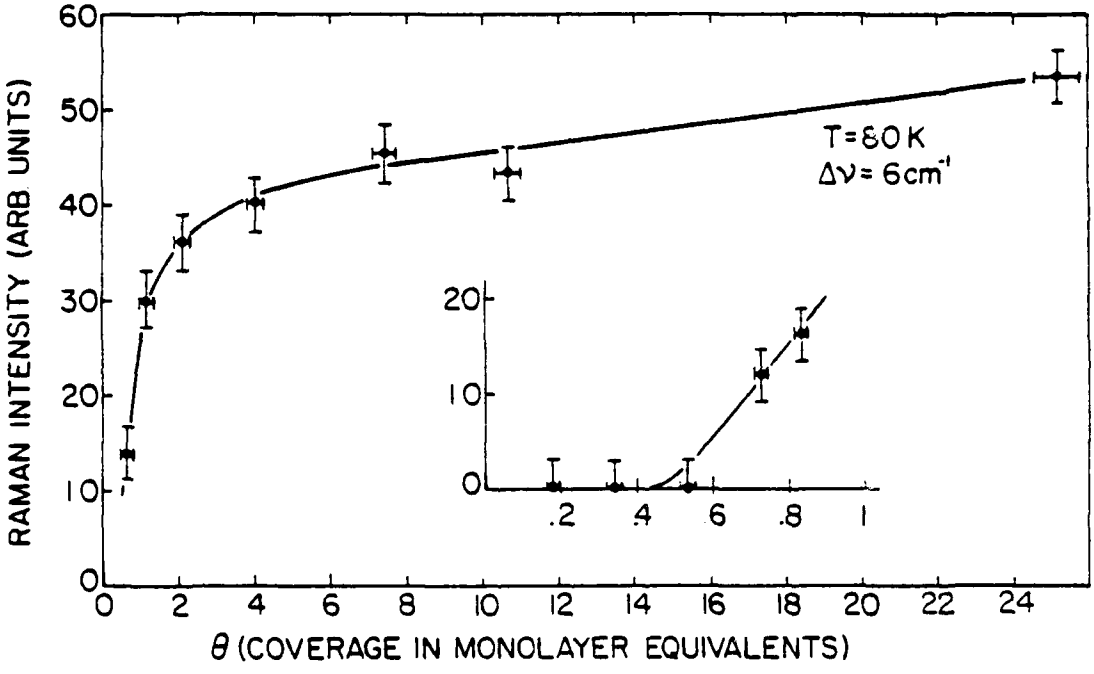

FIG 7
Demuth et al

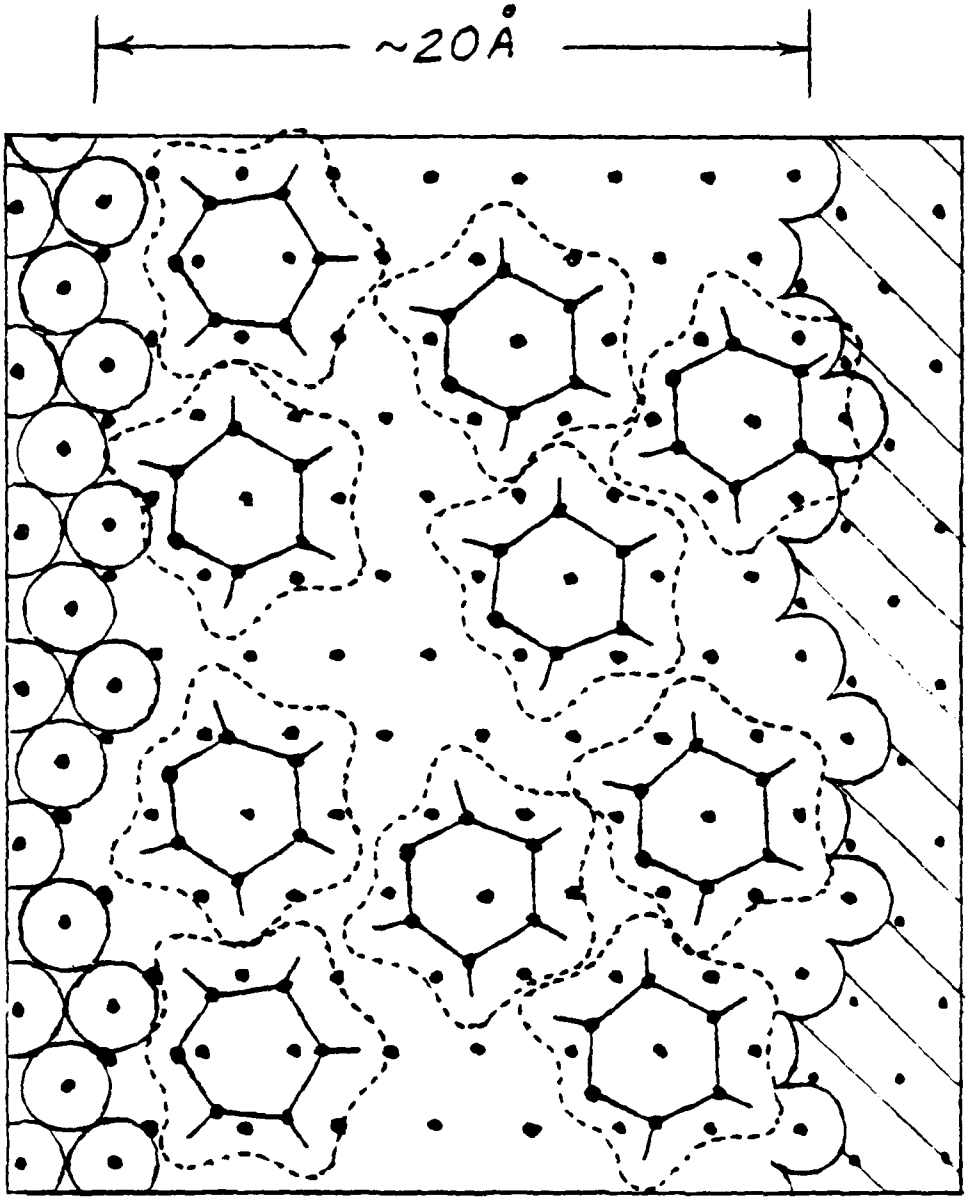

FIG 5
Dolmatch et al

SP472-3/A1

472:GAN:716:ddc
78u472-608

TECHNICAL REPORT DISTRIBUTION LIST, GEN

	No. Copies
Office of Naval Research Attn: Code 472 800 North Quincy Street Arlington, Virginia 22217	2
ONR Branch Office Attn: Dr. George Sandoz 536 S. Clark Street Chicago, Illinois 60605	1
ONR Area Office Attn: Scientific Dept. 715 Broadway New York, New York 10003	1
ONR Western Regional Office 1030 East Green Street Pasadena, California 91106	1
ONR Eastern/Central Regional Office Attn: Dr. L. H. Peebles Building 114, Section D 666 Summer Street Boston, Massachusetts 02210	1
Director, Naval Research Laboratory Attn: Code 6100 Washington, D.C. 20390	1
The Assistant Secretary of the Navy (RE&S) Department of the Navy Room 4E736, Pentagon Washington, D.C. 20350	1
Commander, Naval Air Systems Command Attn: Code 310C (H. Rosenwasser) Department of the Navy Washington, D.C. 20360	1
Defense Technical Information Center Building 5, Cameron Station Alexandria, Virginia 22314	12
Dr. Fred Saalfeld Chemistry Division, Code 6100 Naval Research Laboratory Washington, D.C. 20375	1
U.S. Army Research Office Attn: CRD-AA-IP P.O. Box 1211 Research Triangle Park, N.C. 27709	1
Naval Ocean Systems Center Attn: Mr. Joe McCartney San Diego, California 92152	1
Naval Weapons Center Attn: Dr. A. B. Amster, Chemistry Division China Lake, California 93555	1
Naval Civil Engineering Laboratory Attn: Dr. R. W. Drisko Port Hueneme, California 93401	1
Department of Physics & Chemistry Naval Postgraduate School Monterey, California 93940	1
Dr. A. L. Slafkosky Scientific Advisor Commandant of the Marine Corps (Code RD-1) Washington, D.C. 20380	1
Office of Naval Research Attn: Dr. Richard S. Miller 800 N. Quincy Street Arlington, Virginia 22217	1
Naval Ship Research and Development Center Attn: Dr. G. Bosmajian, Applied Chemistry Division Annapolis, Maryland 21401	1
Naval Ocean Systems Center Attn: Dr. S. Yamamoto, Marine Sciences Division San Diego, California 91232	1
Mr. John Boyle Materials Branch Naval Ship Engineering Center Philadelphia, Pennsylvania 19112	1

TECHNICAL REPORT DISTRIBUTION LIST, GEN

	No. Copies
Dr. Rudolph J. Marcus Office of Naval Research Scientific Liaison Group American Embassy APO San Francisco 96503	1
Mr. James Kelley DTNSRDC Code 2803 Annapolis, Maryland 21402	1

TECHNICAL REPORT DISTRIBUTION LIST, 056

	No. Copies
Dr. D. A. Vroom IRT P.O. Box 80817 San Diego, California 92138	1
Dr. G. A. Somorjai Department of Chemistry University of California Berkeley, California 94720	1
Dr. L. N. Jarvis Surface Chemistry Division 4555 Overlook Avenue, S.W. Washington, D.C. 20375	1
Dr. J. B. Hudson Materials Division Rensselaer Polytechnic Institute Troy, New York 12181	1
Dr. John T. Yates Surface Chemistry Section National Bureau of Standards Department of Commerce Washington, D.C. 20234	1
Dr. Theodore E. Madey Surface Chemistry Section Department of Commerce National Bureau of Standards Washington, D.C. 20234	1
Dr. J. M. White Department of Chemistry University of Texas Austin, Texas 78712	1
Dr. Keith H. Johnson Department of Metallurgy and Materials Science Massachusetts Institute of Technology Cambridge, Massachusetts 02139	1
~~Dr. J. E. Demuth IBM Corpertion Thomas J. Watson Research Center P.O. Box 218 Yorktown Heights, New York 10598~~	1
Dr. C. P. Flynn Department of Physics University of Illinois Urbana, Illinois 61801	1
Dr. W. Kohn Department of Physics University of California (San Diego) LaJolla, California 92037	1
Dr. R. L. Park Director, Center of Materials Research University of Maryland College Park, Maryland 20742	1
Dr. W. T. Peria Electrical Engineering Department University of Minnesota Minneapolis, Minnesota 55455	1
Dr. Narkis Tzoar City University of New York Convent Avenue at 138th Street New York, New York 10031	1
Dr. Chia-wei Woo Department of Physics Northwestern University Evanston, Illinois 60201	1
Dr. D. C. Mattis Polytechnic Institute of New York 333 Jay Street Brooklyn, New York 11201	1
Dr. Robert M. Hexter Department of Chemistry University of Minnesota Minneapolis, Minnesota 55455	1
Dr. R. P. Van Duyne Chemistry Department Northwestern University Evanston, Illinois 60201	1

TECHNICAL REPORT DISTRIBUTION LIST, 056

	No. Copies
Dr. M. G. Lagally Department of Metallurgical and Mining Engineering University of Wisconsin Madison, Wisconsin 53706	1
Dr. Robert Gomer Department of Chemistry James Franck Institute 5640 Ellis Avenue Chicago, Illinois 60637	1
Dr. R. G. Wallis Department of Physics University of California, Irvine Irvine, California 92664	1
Dr. D. Ramaker Chemistry Department George Washington University Washington, D.C. 20052	1
Dr. P. Hansma Chemistry Department University of California, Santa Barbara Santa Barbara, California 93106	1
Dr. P. Hendra Chemistry Department Southhampton University England S09JNH	1
Professor P. Skell Chemistry Department Pennsylvania State University University Park, Pennsylvania 16802	1
Dr. J. C. Hemminger Chemistry Department University of California, Irvine Irvine, California 92717	1
Dr. Martin Fleischmann Department of Chemistry Southampton University Southampton 509 5NH Hampshire, England	1
Dr. J. Osteryoung Chemistry Department SUNY, Buffalo Buffalo, New York 14214	1
Dr. G. Rubloff I.B.M. Thomas J. Watson Research Center P. O. Box 218 Yorktown Heights, New York 10598	1
Dr. J. A. Gardner Department of Physics Oregon State University Corvallis, Oregon 97331	1
Dr. G. D. Stein Mechanical Engineering Department Northwestern University Evanston, Illinois 60201	1
Dr. K. G. Spears Chemistry Department Northwestern University Evanston, Illinois 60201	1
Dr. R. W. Plummer University of Pennsylvania Department of Physics Philadelphia, Pennsylvania 19104	1
Dr. E. Yeager Department of Chemistry Case Western Reserve University Cleveland, Ohio 41106	2
Professor George H. Morrison Cornell University Department of Chemistry Ithaca, New York 14853	1
Professor N. Winograd Pennsylvania State University Chemistry Department University Park, Pennsylvania 16802	1
Professor Thomas F. George The University of Rochester Chemistry Department Rochester, New York 14627	1